

Reflection Coefficient Measurement through the Implementation of Wideband Multi-Port Reflectometer with Error Correction for Microwave Imaging Application of Human Head

Rashidah Che Yob^a, Norhudah Seman^{a*}

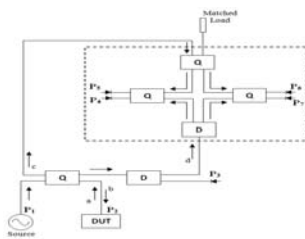
^aWireless Communication Centre (WCC), Universiti Teknologi Malaysia, 81310 UTM Johor Bahru, Johor, Malaysia

*Corresponding author: huda@fke.utm.my

Article history

Received :12 July 2012
Received in revised form:
4 April 2013
Accepted :15 April 2013

Graphical abstract



Abstract

This article presents the reflection coefficient measurement by using a wideband multi-port reflectometer for microwave imaging application of human head. The configuration of the proposed wideband multi-port reflectometer is formed by passive components, which are four couplers and two power dividers operating from 1 to 6 GHz. The investigation is successfully done through simulation using the Agilent's Advanced Design Systems (ADS) software and practical measurement in laboratory. An error correction method with three standards of match, open and short load is then applied to the constructed wideband multi-port reflectometer to remove its imperfect characteristics. The wideband characteristics of proposed reflectometer are analyzed and verified across the designated frequency band. Its operation in reflection coefficient is tested with the chosen device under test (DUT).

Keywords: Passive component; coupler; power divider; multi-port reflectometer; reflection coefficient; wideband; error correction

Abstrak

Artikel ini membentangkan pengukuran pekali pantulan dengan menggunakan reflektometer jalur lebar pelbagai-terminal untuk aplikasi mikro pengimejan kepala manusia. Konfigurasi reflektometer jalur lebar pelbagai-terminal yang dicadangkan dibentuk oleh komponen pasif, iaitu empat pengganding dan dua pembahagi kuasa yang beroperasi dalam julat frekuensi 1 sehingga 6 GHz. Kajian ini berjaya dilakukan melalui simulasi menggunakan perisian Sistem Rekabentuk Agilent (ADS) dan ukuran praktikal di dalam makmal. Kemudiannya, satu kaedah pemetulan ralat dengan tiga piawaian iaitu beban sepadan, terbuka dan pintas diaplikasikan kepada reflektometer jalur lebar pelbagai-terminal untuk menghapuskan ciri-ciri tidak sempurnanya. Ciri-ciri reflektometer jalur lebar yang dicadangkan dianalisis dan disahkan di sepanjang frekuensi yang ditetapkan. Operasinya di dalam pengukuran pekali pantulan diuji dengan peranti (DUT) yang dipilih.

Kata kunci: Komponen pasif; pengganding; pembahagi kuasa; reflektometer pelbagai-terminal; pekali pantulan; jalur lebar; pemetulan ralat

© 2013 Penerbit UTM Press. All rights reserved.

1.0 INTRODUCTION

The brain stroke is stated as third main cause of the death in worldwide [5-12] and particularly in Malaysia [10] after heart disease and cancer such as lung, stomach, liver, and breast cancer [12]. According to World Health Organization (WHO) [12], each year about 15 million people worldwide suffer from stroke attack and one-third of these people die and another one-third of them are suffering permanent disability. Anyone can suffer brain stroke regardless age and gender including children, but most of them are adults. In addition to that, six new cases of stroke occur every hour with an average of 110 people dying daily and around 52 thousand people suffer from stroke every

year in Malaysia [11]. Therefore, a significant interest has been shown in applying microwave imaging technique to image human head as an alternative to X-ray mammography and microwave resonance imaging (MRI).

In microwave imaging, a microwave image is obtained by generating and receiving short pulses for various locations of the probe antenna at many frequencies and viewing angles [2]. By applying the step-frequency pulse synthesis technique, such short pulse can be produced [3]. In this technique, measurement can be carried out in the frequency domain between 0.3 and 300 GHz using low-levels of the electromagnetic energy [4]. Then, the space/time domain representation can be achieved by using an Inverse Fast Fourier Transform (IFFT). Particularly, selecting

the optimal spectrum to be used in microwave imaging systems is very important in human head imaging in which to couple

There is a tradeoff between two important factors in imaging that need to be considered, which are resolution and penetration depth. Resolution is related to the signal bandwidth and velocity of propagation. Meanwhile, penetration depth tends to be longer with longer wavelength. Therefore, longer penetration depth can be obtained at low frequencies. For the case of human head, selection of the optimal spectrum requires the consideration of the brains is surrounded by high contrast dielectric shield comprising of the skin, skull and cerebral spinal fluid [4]. By considering these factors, the chosen frequency range is from 1 to 6 GHz. Figure 1 shows the example of the microwave imaging setup of the human head, which consist of transmitter/receiver, antenna and phantom [13].

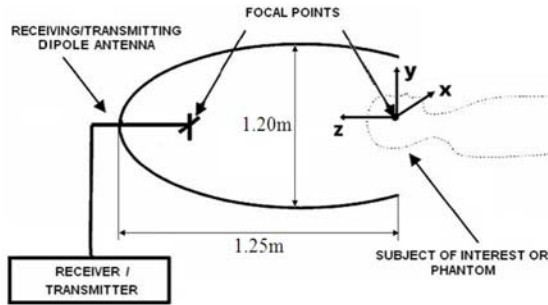
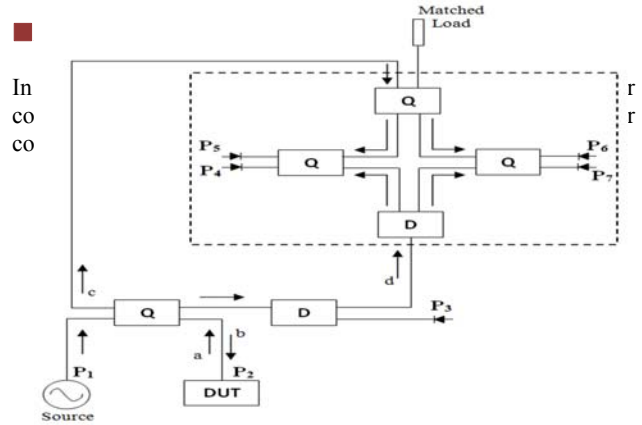


Figure 1 Microwave imaging setup of human head [13]

Commonly, a conventional Vector Network Analyzer (VNA) has been used in working prototypes of the microwave imaging systems as the transmitter and receiver, but it has large size and high cost [14]. While, the demand of many applications today requires compact size and low-cost measurement instruments. Therefore, a wideband multi-port reflectometer is proposed to be implemented in determination of the reflection coefficient that accomplished such measurement of reflected and incident waves at measurement port [14-15].

In so-called real-time mode operation, the multi-port reflectometer is operating in non-ideal manner. This imperfect behavior needs to be corrected by applying a suitable error correction procedure in order to offer accurate measurement of any DUT. Therefore, a calibration or can be known as an error correction with three standards of match, open and short-circuit is proposed to be applied to the wideband reflectometer within the frequency range of 1 to 6 GHz. The investigation will involve two stages, which are simulation and practical measurement. The simulation is performed via the use of Agilent's Advanced Design Systems (ADS) simulator. While, at measurement stage, 90° hybrid couplers and two-way in-phase power dividers are used to integrate the reflectometer. The characteristic performances for the wideband multi-port reflectometer will be evaluated based on S-parameters (transmission coefficients and return losses), phase characteristics and power circle centers (*q*-points). Meanwhile, its operation will be assessed in term of reflection coefficient measurement of DUTs with and without the implementation of error correction procedure.

electromagnetic energy into brain matter [4].



A microwave source and device under test (DUT) are connected to Port 1 and 2, accordingly. Variable 'a' and 'b' represent a reflected signal from DUT and incident signal to DUT, accordingly. Meanwhile, Port 3 to 7 are terminated by four scalar power detectors. The part of the multi-port reflectometer in Figure 2 enclosed with the broken line is called as complex ratio measuring unit (CRMU) or known as correlator.

In simulation stage, the proposed wideband multi-port reflectometer in this article is constructed by three-section coupled-line couplers and two-stage Wilkinson power dividers. The schematic circuits of these two components that accomplished by using Agilent's Advance Design Systems (ADS) simulator are presented in Figure 3 and 4, respectively.

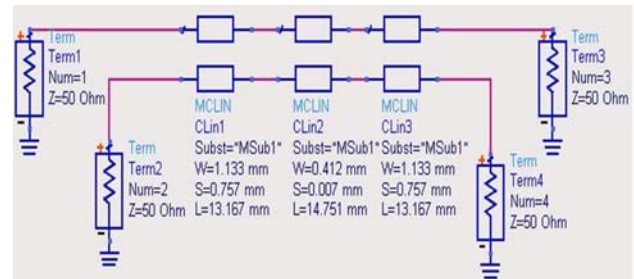


Figure 3 Three-section coupled-line coupler circuit

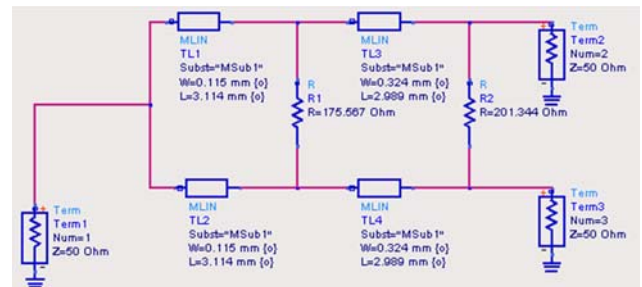


Figure 4 Two-stage Wilkinson power divider circuit

Concerning the frequency range from 1 to 6 GHz, the amplitude response of S_{21} and S_{31} are $-3 \text{ dB} \pm 2 \text{ dB}$ for the three-section coupled-line coupler. It demonstrates the return loss and isolation better than 17 dB and 16 dB, respectively. While, for the phase difference between S_{21} and S_{31} is $-90^\circ \pm 5^\circ$.

Meanwhile, the amplitude response of S_{21} and S_{31} are $-3 \text{ dB} \pm 2 \text{ dB}$ for the two-stage Wilkinson power divider. Its return loss and isolation are greater than 10 dB and 15 dB, accordingly. Whilst, the phase difference between output at Port 2 and Port 3 is almost perfect at 0° . The S-parameter and phase characteristic performances of the three-section coupled-line coupler and two-stage Wilkinson power are comparable to theoretical and met the required specification across the designated frequency band.

Whilst, for the measurement stage; the proposed wideband multi-port reflectometer is constructed by using real components. Then, the experiment is conducted in the laboratory with the use of vector network analyzer (VNA). The used Krytar 90° hybrid coupler, Aeroflex two-way in-phase power divider and cable are shown in Figure 5. The coupling of the 90° hybrid coupler is 3 dB and its isolation is more than 20 dB with 90° phase different across the frequency range of 1 to 12.4 GHz. Meanwhile, the isolation of the two-way in-phase power divider is more than 16 dB with 0° phase difference and equal power division between two output ports.

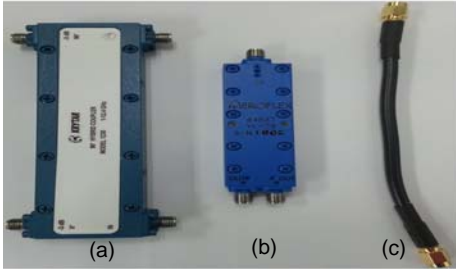


Figure 5 The components used to form the proposed wideband multi port reflectometer: (a) coupler (b) power divider and (c) cable

By assuming an ideal operation of the coupler and power divider with mathematical derivation from their signal flow [14], it can be shown that the reflection coefficient (Γ) of the DUT for the configuration in Figure 2 is:

$$\Gamma = \frac{a}{b} = \Gamma_1 + j\Gamma_2 = \frac{(P_4 - P_5) + j(P_6 - P_7)}{P_3} \quad (1)$$

where, Γ_1 , Γ_2 and P_i ($i = 4, 5, 6, 7$) are the real and imaginary component of the complex reflection coefficient, and measured power at output ports, respectively. This notation i indicates the output port of reflectometer. While, a reflected signal and an incident signal of DUT are denoted by variable 'a' and 'b', respectively. Then, by assuming square-law operation of the detectors, an equivalent representation of Γ in (1) can be obtained from the scattering parameters of the wideband multi-port reflectometer as the following equation (2):

$$\Gamma = \frac{(|S_{41}|^2 - |S_{51}|^2) + j(|S_{61}|^2 - |S_{71}|^2)}{|S_{31}|^2} \quad (2)$$

Consequently, the output voltage at Port 4 to 7 can be written in the form of the incident signal (b), reflection coefficient (Γ) and centre of the power circle (q -point) as in following equation (3) [18]. Where, in this equation the q -point is denoted by variable q_i with $i = 4, 5, 6, 7$.

$$\begin{aligned} V_4 &= -\frac{b}{2\sqrt{2}}(\Gamma - q_4) \\ V_5 &= \frac{jb}{2\sqrt{2}}(\Gamma - q_5) \\ V_6 &= \frac{b}{2\sqrt{2}}(\Gamma - q_6) \\ V_7 &= -\frac{jb}{2\sqrt{2}}(\Gamma - q_7) \end{aligned} \quad (3)$$

Meanwhile, the value of the q -point (q_i) can be determined from the next following equation (4). Then, the expression (5) is representing the phase characteristics of the q -point (q_i) that referred against q_4 [18]:

$$q_i = -\frac{S_{i1}}{S_{i2}S_{21} - S_{i1}S_{22}} \quad (4)$$

$$\text{phase}(q_{\Delta}) = \text{phase}(q_i) - \text{phase}(q_4) \quad (5)$$

where, the ideal values of q_i ($i = 4, 5, 6, 7$) for the chosen reflectometer configuration are 1, -1, $-j1$ and $j1$, accordingly. Hence, these ideal q_i have similar magnitude of 1 with 90° phase separation.

3.0 THE CHARACTERISTICS OF WIDEBAND MULTI-PORT REFLECTOMETER

The concerned characteristics of the wideband multi-port reflectometer are return losses, transmission coefficients, phase characteristics and centre of power circles (q -points). The investigation of the wideband multi-port reflectometer will be started with S-parameter in term of return loss and transmission coefficient before the other considered characteristics.

The simulated and measured return losses and transmission coefficients of the wideband multi-port reflectometer are plotted in Figure 6 and 7. The notation 's' and 'm' are used to denote the simulation and measurement parameters, respectively.

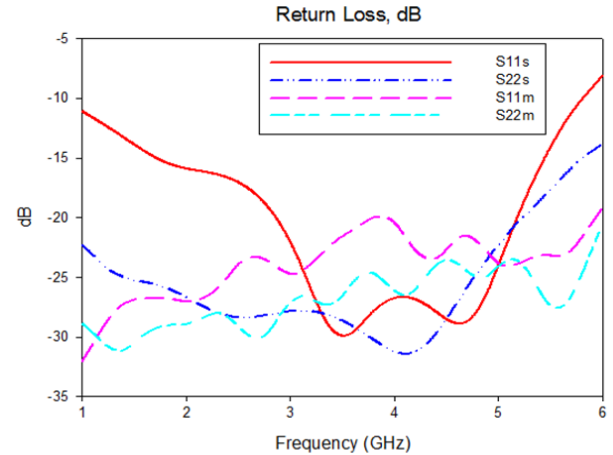


Figure 6 Simulated (s) and measured (m) return loss of the wideband multi-port reflectometer at Port 1 and 2

Concerning the frequency range from 1 to 6 GHz, the simulated return loss at Port 1 and 2 in Figure 6 show S_{11s} and S_{22s} are less than -10 dB and -16 dB, respectively. While, the measured the return loss at Port 1 and 2 depict S_{11m} and S_{22m} are less than -20 dB and -22 dB, accordingly. With regard to the obtained return loss results from simulation and measurement, it

can be noted that measured reflectometer, which formed by coupler and power divider in Figure 5 offers better performance than the one from simulation in ADS.

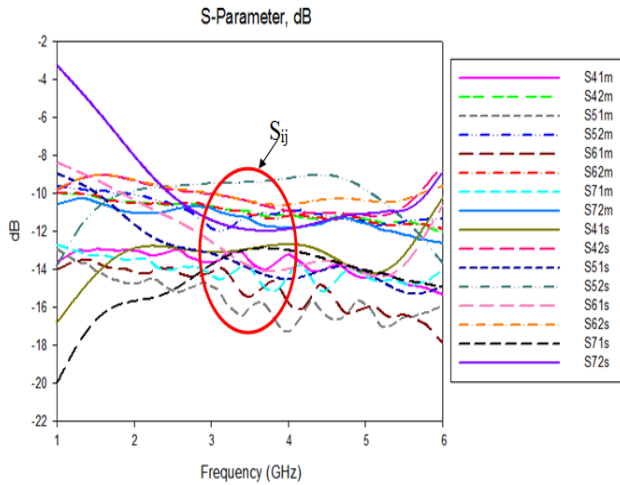


Figure 7 Simulated (s) and measured (m) transmission coefficient (S_{ij}) of the wideband multi-port reflectometer where $i = 4, 5, 6, 7$ and $j=1, 2$

Next, the transmission coefficients, S_{ij} referenced to Port 1 and Port 2 are assessed across the designated frequency range. Based on the obtained results in Figure 7, it can be summarized that the simulated transmission coefficients, S_{ijs} are $-13 \text{ dB} \pm 2 \text{ dB}$. The measured transmission coefficients, S_{ijm} show slightly worst performance compared to the simulation with $-14 \text{ dB} \pm 2 \text{ dB}$. The most deviation can be noticed at the lower end of the frequency range, which is around 1 to 2 GHz.

Then, the following investigation of the wideband multi-port reflectometer is concerning its phase characteristics. The phase characteristics of the transmission coefficients for the wideband multi-port reflectometer are referenced against S_{41} and S_{42} as presented in Figure 8 and 9, respectively.

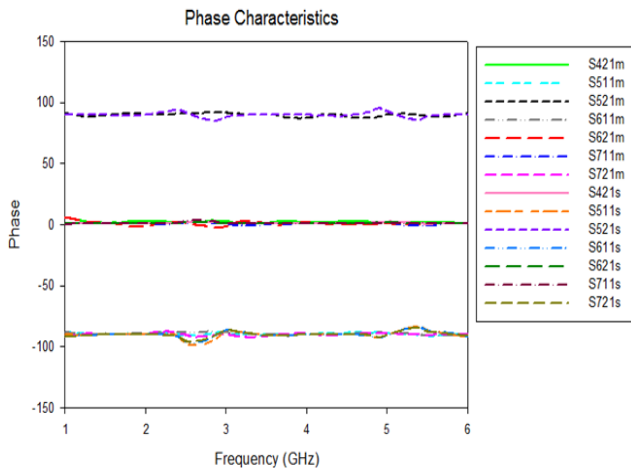


Figure 8 Simulated (s) and measured (m) phase characteristics of the wideband multi-port reflectometer referenced to phase S_{41} where $S_{\Delta ij}$ (degree) = S_{ij} (degree) - S_{41} (degree) with $i = 4, 5, 6, 7$; and $j = 1, 2$

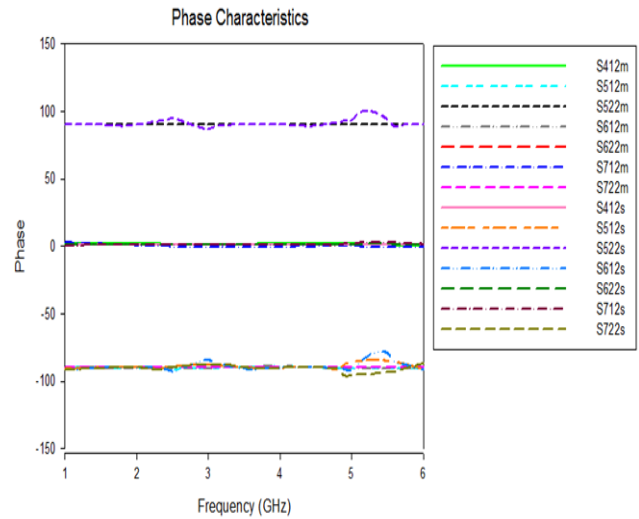


Figure 9 Simulated (s) and measured (m) phase characteristics of the wideband multi-port reflectometer referenced to phase S_{42} where $S_{\Delta ij}$ (degree) = S_{ij} (degree) - S_{41} (degree) with $i = 4, 5, 6, 7$; and $j = 1, 2$

The simulated and measured phase characteristics of the wideband multi-port reflectometer that plotted in Figure 8 and 9 shows the referenced phase characteristics are stay approximately at 0° , -90° and 90° cross the frequency band between 1 and 6 GHz. The obtained results of the phase characteristics for both simulation and measurement show an agreeable good wideband performance.

The next concern is to investigate the characteristics of the power circle centre (q -points) of the wideband multi-port reflectometer. The obtained results of the power circle centre (q -points) are computed using equation (4) and presented in magnitude and phase form. The magnitude and phase characteristics of the power circle centre (q -points) are illustrated in Figure 10 and 11, respectively.

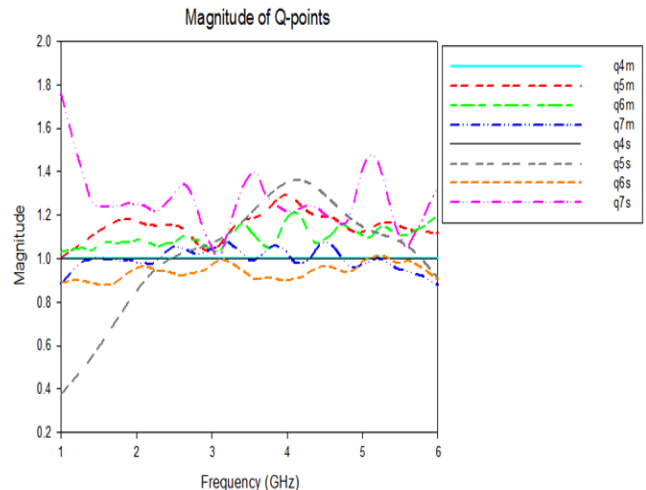


Figure 10 Simulated (s) and measured (m) magnitude of the power circle centre (q -points) of the wideband multi-port reflectometer

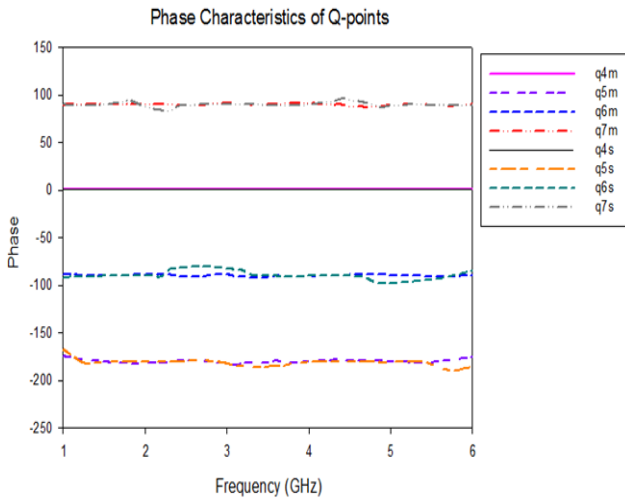


Figure 11 Simulated (s) and measured (m) phase characteristics of the power circle centre (*q*-points) of the wideband multi-port reflectometer

As can be seen, Figure 10 indicates the simulated magnitudes of the power circle centres (*q*-points) for the wideband multi-port reflectometer are approximately 1 ± 0.5 across the frequency range between 2 and 6 GHz. At lower end of designated frequency band between 1 and 2 GHz, the most deviated performance can be observed compared to ideal value of 1. While, the measured magnitude of the power circle centres (*q*-points) for the wideband multi-port reflectometer are approximately 1 ± 0.3 among the operating frequency range between 1 and 6 GHz. The measured magnitude of the power circle centres (*q*-points) shows a better performance compared to simulated responses.

Meanwhile, Figure 11 points out the simulated and measured phase characteristics of the power circle centre (*q*-points) of the wideband multi-port reflectometer of $q_{\Delta 4}$ to $q_{\Delta 7}$ are around 0° , -180° , -90° and 90° , respectively. These phase characteristics are computed by using equation (5).

Based on the investigation of the characteristic performances for the wideband multi-port reflectometer that obtained through simulation and measurement, it can be noted the wideband multi-port reflectometer has achieved a comparable good wideband performance. Thus, it can be used as alternative measurement instrument in the measurement of reflection coefficient of any DUT. Where, its operation will be tested with the implementation of the proposed error correction procedure.

4.0 REFLECTOMETER ERROR CORRECTION AND ITS VERIFICATIONS

Even though the proposed multi-port reflectometer shows good wideband performance but it operates in non-error-free state. Therefore, with regard to the imperfect operation of the wideband multi-port reflectometer observed in so-called real mode; there is a requirement to implement a calibration or known as error correction. In general, a six to seven-port reflectometer requires at least five calibration standards in order to determine its unknown complex describing its operation [16-17]. However, for the chosen configuration of the wideband multi-port reflectometer; a calibration or error correction procedure using only three standards is proposed to be used. Similar procedure is employed for the conventional four-port

reflectometer and vector network analyzer (VNA) [14]. Basically, this error correction procedure applies the concept of the one-port error model with three standards of match, open and short as presented in Figure 12 [18].

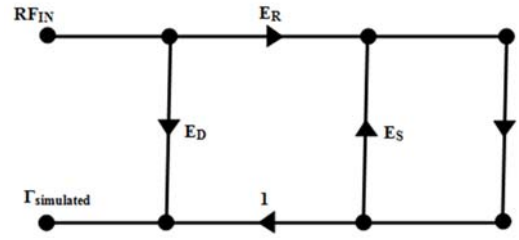


Figure 12 One-port error model with three standards [18]

Referring to the one-port error model with three standards illustrated in Figure 12, the corrected reflection coefficient can be derived as in expression (6) [18]:

$$\Gamma_{corrected} = \frac{\Gamma_{measured} - E_D}{E_R + E_S(\Gamma_{measured} - E_D)} \tag{6}$$

where E_D , E_R and E_S are directivity, reflection signal path and source match error, respectively. These errors can be calculated from the following equation (7) to (9) [18]:

$$E_D = \Gamma_{measured}^{MATCH} \tag{7}$$

$$E_S = \frac{2\Gamma_{measured}^{MATCH} - \Gamma_{measured}^{OPEN} - \Gamma_{measured}^{SHORT}}{\Gamma_{measured}^{SHORT} - \Gamma_{measured}^{OPEN}} \tag{8}$$

$$E_R = (1 - E_S) \left(\Gamma_{measured}^{OPEN} - \Gamma_{measured}^{MATCH} \right) \tag{9}$$

The proposed one-port error correction is applied to the wideband reflectometer using match, open and short-circuit standard with equation (6) to (9). The equation (1) or (2) is used to compute the uncorrected Γ of the chosen DUT while the corrected one is determined using (6). In the simulation stage, the investigation of reflection coefficients with different DUTs of match (50Ω), open-circuit, short-circuit, 5, 10, 25, 40, 45, 55, 100 and 950Ω are performed. These DUTs are connected to Port 2 of the wideband multi-port reflectometer. The simulated results of the uncorrected magnitude reflection coefficients for the selected loads prior to the error correction procedure is performed are shown in Figure 13.

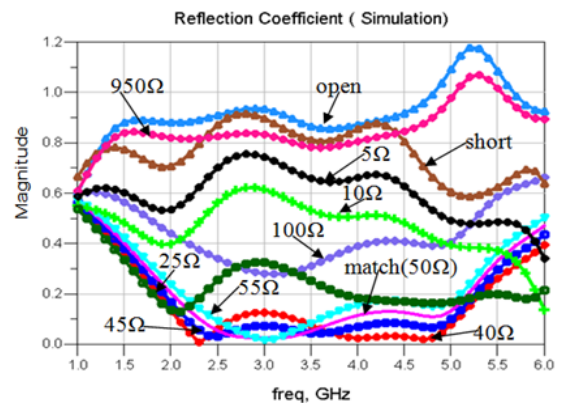


Figure 13 Simulated results of uncorrected reflection coefficients (Γ) of different DUTs

In theory, the ideal value of the magnitude reflection coefficient for match, open and short-circuit is 0, 1 and -1, respectively. As observed from the Figure 13, the simulated magnitude Γ of match load is around 0 to 0.5. While, for open circuit; the simulated magnitude Γ oscillates between 0.3 and 0.9. Then, when short-circuit is connected to Port 2 as DUT, the simulated magnitude Γ is between 0.5 and 1.1. These deviations from the ideal values also can be noted from the obtained magnitude Γ of the rest DUTs. These simulated results of the magnitude Γ show that the wideband multi-port reflectometer is not operating in the error-free state condition. Therefore, the error correction procedure should be applied to remove these imperfect characteristics of the wideband multi-port reflectometer.

The simulated results of corrected reflection coefficients (Γ) for the chosen DUTs are presented in next following Figure 14. As can be observed in Figure 14, the simulated magnitude Γ for each evaluated loads of the DUT is approximately around its ideal value. But, there have some point that still can be improved to perfectly remove the error of the wideband multi-port reflectometer such as at 1 GHz for 25 Ω , 100 Ω and 950 Ω .

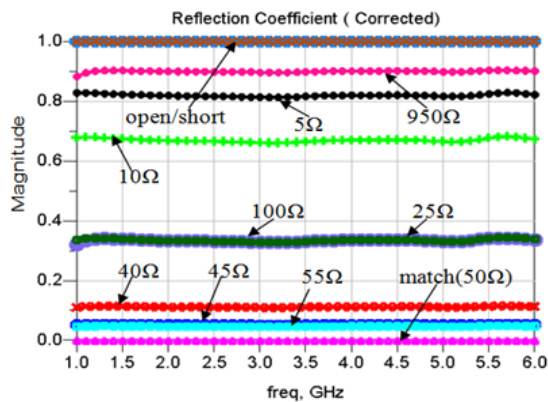


Figure 14 Corrected results of the simulated reflection coefficients (Γ) of a number of DUTs from the proposed wideband multi-port reflectometer

Further investigation of reflectometer operation in reflection coefficient is carried out in laboratory. Three standard loads of Huber+Suhner match, Midwest Microwave open and POMONA short-circuit as shown in Figure 15 are used in the error correction procedure. While, an unknown load, which fabricated using Rogers RO4003C substrate with dielectric constants of 3.38, thickness of 0.508 mm and 17 μm conductor coating as photographed in Figure 16 is applied as DUT. The unknown load consists of a microstrip line and slotline at the top and bottom layer, respectively.

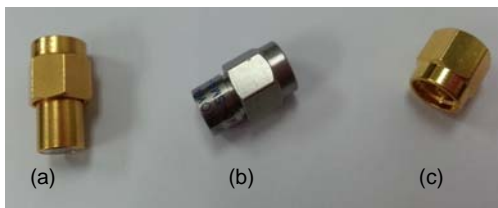


Figure 15 The photography of the standard load terminations: (a) match (b) open and (c) short

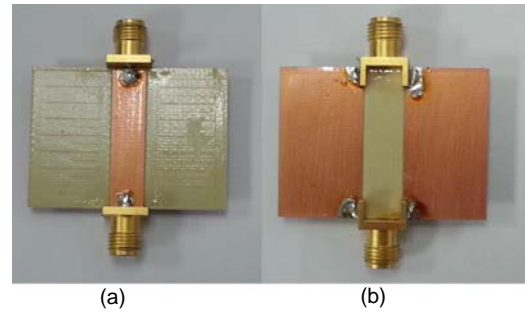


Figure 16 The photography of the unknown load: (a) front view and (b) back view

Similar to the process in simulation stage, the uncorrected of measured unknown load reflection coefficient is computed using simple mathematical equation (1) or (2). Then, with the information of this uncorrected reflection coefficient and errors from (7) to (9), the corrected reflection coefficient of unknown load can be obtained from (6). Figure 17 shows the comparison of uncorrected Γ , corrected Γ and measured Γ from VNA of the unknown load. The notation 'R', 'VNA' and 'corrected' refer to uncorrected, measured from VNA and corrected result, accordingly.

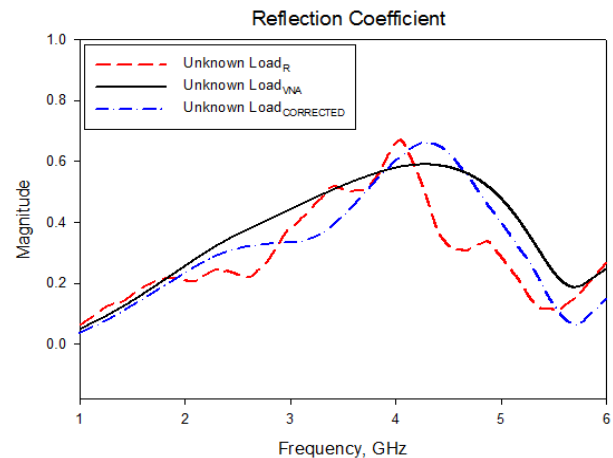


Figure 17 The comparison of uncorrected Γ , corrected Γ and measured Γ from VNA of the unknown load

With regard to the result of the reflection coefficient obtained using VNA, the magnitude Γ is approximately around 0.02 and it rises to 0.55 at 4 GHz. Then, it gradually decrease with lowest value of 0.18 at 5.7 GHz. After that, it slightly increase to 0.25 at 6 GHz. Meanwhile, the magnitude of the uncorrected Γ that determined by using the proposed wideband multi-port indicates non-linear increment and reduction across the frequency band, but it still closely following the pattern shown by the one from VNA with slightly different magnitude Γ . The maximum difference of 0.25 can be observed at 4.5 GHz. Then, for the case of corrected magnitude Γ after the error correction procedure is performed demonstrates close performance to the one from VNA from 1 to 2.5 GHz. Unfortunately, the next following frequency range is unsuccessfully to be corrected due to the overlapping phases of the used standards in the error correction procedure. Figure 18 presents the overlapping phase that occurred from the used standard loads.

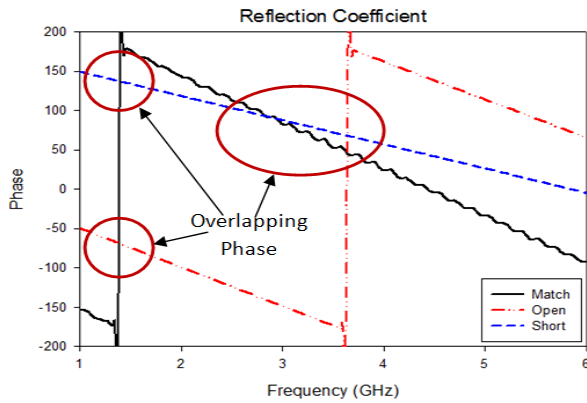


Figure 18 The overlapping phase characteristics of the reflection coefficients for the used standards in error correction procedure

With overlapping phase characteristics of the used standards loads; the error correction procedure is unable to remove the imperfect characteristics of the wideband reflectometer. Therefore, inaccurate performance is expected to be occurred at some of frequency range. This overlapping phase of used standards is happened for all wideband operation. Consequently, to remove the effect of overlapping phase characteristic, it is suggested to adapt the least mean square (LMS) technique with the proposed error correction method.

5.0 CONCLUSION

The reflection coefficient measurement by using a wideband multi-port reflectometer for microwave imaging application of human head has been presented. The characteristics and operations of the wideband multi-port reflectometer have been demonstrated via the implementation of Agilent's Advanced Design Systems (ADS) simulator and practical measurement in laboratory. An error correction method with three standards has been applied to the constructed wideband multi-port reflectometer to remove its imperfect characteristics. Unfortunately, at some frequency range, the reflectometer operation in reflection coefficient measurement is failed to be corrected. This is due to the overlapping phases of the used standards in the error correction procedure, which occur in all wideband operation. Therefore, there is a need to adapt another error correction technique such as least mean square (LMS) together with the one proposed in this article which will be covered in separate article. This will eliminate the overlapping phase effect of the used standards and the wideband reflectometer will be fully corrected.

Acknowledgement

The authors acknowledge the financial support from Ministry of Higher Education Malaysia (MOHE) and Universiti Teknologi Malaysia (UTM) Fundamental Research Grant Scheme (FRGS) with vote number of 4F103 and Research University Grant with vote number of 08J72.

References

- [1] Seman, N., M. E. Bialkowski. 2006. *Design of Wideband Reflectometer for a Microwave Imaging System*. Microwave, Radar & Wireless Communication International Conference (MIKON).
- [2] Khor, W. C., M. E. Bialkowski, S. Crozier. 2005. *Microwave Imaging using Planar Scanning Systems with Step-Frequency Synthesized Pulse*. Proc. APMC2005: Vol. 1.
- [3] Choi, M. K., M. Zhao, S.C. Hagness, D.W. van der Weide. 2005. Compact Mixer-Based 1-12 GHz Reflectometer. *IEEE Microwave and Wireless Components Letters*. 15(11).
- [4] Ireland, D., M. E. Bialkowski. 2010. *Feasibility Study on Microwave Stroke Detection using a Realistic Phantom and the FDTD Method*. Proceedings of Asia-Pacific Microwave Conference.
- [5] Ireland, D., M. E. Bialkowski. 2011. Microwave Head Imaging for Stroke Detection. *Progress in Electromagnetics Research M*. 21: 163-175.
- [6] Mohammed, B. J., A. M. Abbosh, P. Henin, P. Sharpe. 2012. *Head Phantom for Testing Microwave Systems for Head Imaging*. Cairo International Biomedical Engineering Conference (CIBEC).
- [7] Mohammed, B. J., A. M. Abbosh, D. Ireland. 2012. *Stroke Detection based on Variations in Reflection Coefficients of Wideband Antennas*. Antennas and Propagation Society International Symposium (APSURSI).
- [8] Mohammed, B. J., A. M. Abbosh, M. E. Bialkowski. 2011. *Wideband Antenna for Microwave Imaging of Brain*. International Conference on Intelligent Sensors, Sensor Networks and Information Processing (ISSNIP).
- [9] Scapatucci, R., L. D. Donato, I. Catapono, L. Crocco. 2012. A Feasibility Study on Microwave Imaging for Brain Stroke Monitoring. *Progress in Electromagnetics Research B*. 40: 305-324.
- [10] M. Hanip. 2012. National Stroke Registry (NSR): Terengganu and Seberang Jaya Experience. *Medical Journal Malaysia*. 67(3).
- [11] Krishnamoorthy, M. 2007. *Killer Stroke: Six Malaysian Jit Every Hour*. The Star Newspaper. Tuesday, 24 April.
- [12] World Health Organization (WHO). 2004. *The World Health Report*. Geneva, Switzerland.
- [13] Gouzouasis, I. A., I. S. Karanasiou, N. K. Uzunoglu. 2009. *Exploring the Enhancement of the Imaging Properties of a Microwave Radiometry Systems for Possible Functional Imaging using a Realistic Human Head Model*. 4th International Conference Imaging Technology in Bio-Medical Sciences. Medical Images to Clinical Information: Bridging the Gap.
- [14] Bialkowski, M. E., N. Seman. 2010. *Ultra Wideband Microwave Multi-Port Reflectometer in Microstrip-Slot Technology: Operation, Design and Applications*. Advanced Microwave and Millimeter Wave Technologies Semiconductor Devices Circuits and Systems. Vienna: In-Tech.
- [15] Bialkowski, M. E., N. Seman, M. S. Leong, S. P. Yeo. 2008. *Fully Integrated Microwave Reflectometer in Multi-Layer Microstrip-Slot Technology for Ultra Wideband Applications*. 17th International Conference on Microwaves, Radar and Wireless Communication (MIKON).
- [16] Hoer, C. A. 1977. *A Microwave Network Analyzer using Two 6-port Reflectometer*. Microwave Symposium Digest MTT-S International: 77(1).
- [17] Bialkowski, M. E. 1993. Microwave Network Analyzer incorporating a Single Six-port Reflectometer. *AEU International Journal of Electronics and Communications*. 47(3).
- [18] Seman, N. 2010. *Multi-port Reflectometer in Multilayer Microstrip-slot Technology for Ultra-wideband Applications*. Ph.D Dissertation, The University of Queensland, Australia.